About the impact of the Unresolved Resonance Region in Monte Carlo simulations of Sodium Fast Reactors

A. Jiménez-Carrascosa[1*], E. Fridman[2], N. García-Herranz[1], F. Alvarez-Velarde[3], P. Romojaro[3], F. Bostelmann[4]

[1]Department of Energy Engineering, Universidad Politécnica de Madrid (UPM), José Gutiérrez Abascal 2, 28006 Madrid, Spain
[2]Helmholtz-Zentrum Dresden-Rossendorf (HZDR), Bautzner Landstraße 400, 01328 Dresden, Germany
[3]Centro de Investigaciones Energéticas, Medioambientales y Tecnológicas (CIEMAT), Avda. Complutense, 40. 28040 Madrid, Spain
[4]Oak Ridge National Laboratory (ORNL), P.O. Box 2008, Bldg. 5700, Oak Ridge, TN 37831-6170, USA
[*]Corresponding Author, E-mail: antonio.jcarrascosa@upm.es

In the last few years, and within the framework of different European projects, KENO-VI code from SCALE system has been employed to perform detailed continuous-energy Monte Carlo transport calculations for advanced fast reactors. The core characterization of both the sodium-cooled ASTRID and the lead-cooled ALFRED reactors was performed during the FP7 cross-cutting ESNII+ project; more recently, core calculations for the sodium-cooled Superphénix reactor and the improved European Sodium Fast Reactor design were performed within the HORIZON2020 ESFR-SMART project. In all cases, the effective multiplication factor predicted by KENO-VI was systematically higher (around 400-500 pcm) than the values computed by MCNP and Serpent Monte Carlo codes, using the same nuclear data library.

In order to provide insight into the origin of the observed discrepancies, a simplified 2D MOX-fueled SFR pin-cell benchmark has been launched. The multiplication factor, as well as 1-group and VITAMINJ 175-group cross-sections computed by KENO-VI, Serpent and MCNP codes employing ENDF/B-VII.1 data library, have been compared.

Significant differences between KENO-VI and the other codes have been found in the unresolved resonance regions of ^{239}Pu and ^{241}Pu capture and production cross sections, while negligible differences appeared outside those energy ranges. On the other hand, calculations without using probability tables have shown very good agreement. Quantitative comparison is presented and analyzed, along with a discussion of the impact of the probability-table treatment in the three codes for MOX-fueled systems with typical SFR spectrum.

KEYWORDS: Unresolved Resonance Region, Probability Tables, Monte Carlo simulations of SFR

Introduction

The Horizon2020 European project ESFR-SMART (European Sodium Fast Reactor Safety Measures and Research Tools) [1] was launched in September 2017 with the main objective of further enhancing the safety of Generation-IV Sodium Fast Reactors (SFR) and particularly of the commercial-size European Sodium Fast Reactor.

In order to assess the new safety measures implemented in the optimized ESFR core, well-calibrated and validated simulation tools have to be used. Verification and validation of the computational tools and methodologies, along with uncertainty quantification, is then required to give credibility to simulation-based results.

With that goal, and related with the initial core performance assessment of the 3-D heterogeneous ESFR core, several neutronics codes have been employed and widely benchmarked. In particular, results provided by three continuous-energy Monte Carlo codes have been compared: Serpent, MCNP and KENO-VI.

Significant differences in the effective multiplication factor were encountered. KENO-VI predicted an effective multiplication factor around 400-500 pcm higher than the values computed by Serpent and MCNP using the same nuclear data library (ENDF/B-VII.1). An overestimation of reactivity was also predicted by KENO-VI for Superphénix reactor benchmark also in the frame of the ESFR-SMART project [2].

These tools have been previously used for calculation of advanced fast reactors within the framework of different European projects and similar differences were found systematically between KENO-VI and Serpent or MCNP outcomes. Firstly, during ESNII+ project and related to SFR core characterization, ASTRID calculations at End of Cycle (EoC) were performed obtaining a difference in the k_{eff} value of ~400 pcm between KENO-VI and Serpent by using the same nuclear data library (ENDF/B-VII.0) [3]. Secondly and also during ESNII+ project, lead-cooled ALFRED core calculations at Beginning of Cycle (BoC) were conducted and, in this case, a disagreement of ~500 pcm was found between KENO-VI and MCNP using the ENDF/B-VII.1 nuclear data library [4]. On the other hand, within CHANDA project [5], MYRRHA calculations for critical and sub-critical homogeneous models at Beginning of Life (BoL) were performed. In both cases and using the ENDF/B-VII.0 library, core multiplication factors showed a discrepancy around 250 pcm between KENO-VI and MCNP [6].

The objective of this work is to provide insight into the origin of the observed discrepancies. To achieve this goal, a simplified SFR pin-cell benchmark has been launched in order to carry out an exhaustive comparison between the three Monte Carlo codes employing the ENDF/B-VII.1 data library.

In this paper, main results of this simplified benchmark are presented and in-depth analyzed. Initially, the multiplication factor as well as one-group collapsed cross sections evaluated by each have been compared to identify the main contributors to the differences. At the next stage, a detailed inter-comparison of multi-group cross sections of the most important nuclides/reactions has been conducted employing the VITAMINJ 175-group structure. An important effect of the unresolved resonance regions (URR) of some nuclides/reactions cross sections, which leads to the discrepancies on the k_{eff} values predicted by each code, has been detected taking into account the calculations performed by switching off the use of the probability tables.

Probability-Table Method for Unresolved Resonance Region

For certain isotopes at sufficiently high incident neutron energies, there is an energy region where the cross section resonances are practically overlapped not allowing their experimental resolution. This region is known as the unresolved resonance region and it is located between the resolved resonance and continuum regions. Consequently, the structure associated with the URR does not allow a precise description of the neutron cross section values, which must be described by average resonance parameters and statistical distributions over energy.

Detailed Monte Carlo transport simulations must implicitly take into account the important physical phenomena in the unresolved resonance energy region. Typically, the probability table method has been employed in order to account for URR structure preserving the energy self-shielding effects [7]. This method relies on the statistical nature of the resonance parameters in this region and is based on the sampling of pre-generated discrete cross sections values with related energy-discretized probability distributions. During the simulation these discrete data, which are organized in a set of tables, are sampled to obtain the cross section values in the URR.

The effect of the probability-table treatment in various uranium and plutonium benchmarks has been assessed [8], and the systems for which the probability-table method has an important effect have been identified. Here, it is shown that advanced fast reactors, such as the sodium-cooled ASTRID, Superphénix or optimized ESFR or the lead-cooled ALFRED and MYRRHA reactors, are especially sensitive to the unresolved resonance energy region due to the neutron energy spectra in this type of systems.

Monte Carlo simulation tools

As previously stated, this study is based on the calculations performed by the continuous-energy Monte Carlo codes KENO-VI, MCNP and Serpent.

KENO-VI [9] is the three-dimensional Monte Carlo criticality module of SCALE Code System [10], developed and maintained by Oak Ridge National Laboratory (ORNL). In this work, calculations are performed using the continuous-energy AMPX-formatted data provided by SCALE, in its version 6.2.3, based on the ENDF/B-VII.1 library [11]. The effect of the interpolation method implemented to provide problem-dependent temperature corrections is avoided by selecting as benchmark temperatures those for which continuous-energy data are available in SCALE.

MCNP6 [12] is a reference general-purpose, continuous-energy, generalized-geometry and time-dependent Monte Carlo code designed to track many particle types over broad ranges of energies, developed and maintained by Los Alamos National Laboratory. In this work, the ENDF/B-VII.1 based ACE-formatted nuclear data library, processed at CIEMAT with NJOY2016 [13] to the benchmark temperatures, was used for MCNP calculations.

Serpent [14] is a multi-purpose three-dimensional continuous-energy Monte Carlo code, developed at VTT Technical Research Centre of Finland. The Serpent calculations have been performed using ENDF/B-VII.1 based ACE-formatted nuclear data processed at VTT.

Since MCNP shares the ACE data format with Serpent, MCNP calculations have been also performed using the nuclear data library originally processed for Serpent calculations. This case is identified as "MCNP-HZDR" along the paper and it is used to assess the impact of the processing on computed results.

Impact of Unresolved Resonance Region using a simplified SFR pin-cell model

The benchmark exercise is based on a very simplified 2D SFR pin-cell model (see Figure 1) comprising three regions: 1) a MOX-based fuel region (composed of ^{16}O, ^{235}U, ^{238}U, ^{239}Pu, ^{240}Pu, ^{241}Pu, ^{242}Pu and ^{241}Am); 2) a cladding region modeled using a single isotope (^{56}Fe), and 3) the sodium coolant (^{23}Na). The model does not include the central hole as well as the gap between the fuel material and the cladding. Reflective boundary conditions are applied in all directions. Temperatures for ENDF/B-VII.1-based cross-sections are 1200 K for fuel material and 900 K for cladding and sodium.
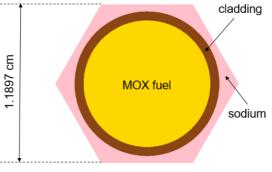

Figure 1: Simplified 2-D SFR pin-cell model.

A first set of the results includes a comparison of both the infinite multiplication factor (k_{inf}) and main one-group collapsed problem-dependent cross sections. In this sense, the computed multiplication factors are compared in Table 1 and the one-group cross sections and their deviations with respect to the Serpent ones are summarized in Figure 2.

Calculation	k_{inf}	$\Delta\rho = (1/k_{ref} - 1/k_{inf})$ [pcm]
Serpent	1.31687(2)	reference
MCNP-HZDR	1.31685(5)	-1
MCNP-CIEMAT	1.31853(5)	96
KENO-VI	1.32607(2)	527

Table 1: Criticality calculations for the pin-cell. The 1σ standard deviation of the Monte Carlo results is given in parentheses.

Regarding the multiplication factor comparison, KENO-VI overpredicts the reactivity with respect to Serpent and MCNP, exhibiting the same behavior observed in the previously mentioned whole core calculations. Comparison of both MCNP results illustrates the impact on reactivity of the different nuclear data processing carried out with NJOY for this benchmark.

The comparison of the one-group cross sections in Figure 2 reveals significant differences for some nuclide reactions. As it can be seen, ^{239}Pu and ^{241}Pu capture and production cross sections can be identified as the major contributors to the deviations. The highest difference corresponds to ^{241}Pu(n, γ) cross section since the value obtained by KENO-VI differs more than 4% to the ones provided by both Serpent and MCNP. In addition, ^{241}Pu(n, f) cross section computed by KENO-VI has a 2.3% difference regarding Serpent and MCNP results. On the other hand, ^{239}Pu(n, γ) and ^{239}Pu(n, f) cross sections provided by KENO-VI differ up to 0.5% with respect to the other codes. Moreover, systematic underestimation of capture reactions for nuclides such as ^{238}U, ^{56}Fe and ^{23}Na can be also observed.
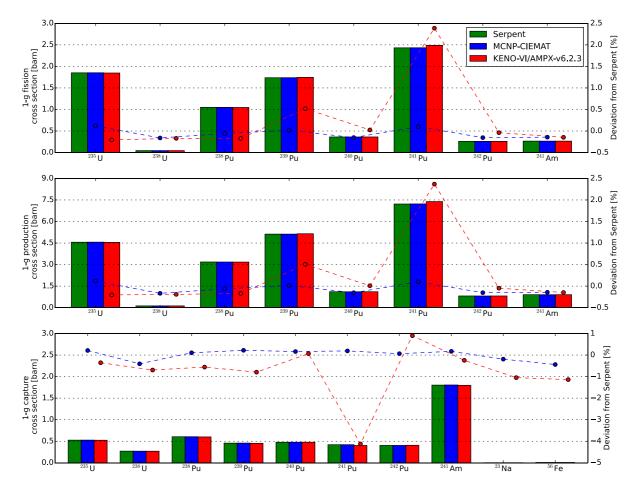

Figure 2. Collapsed one-group cross sections and relative deviations with respect to Serpent (bars refer to 1-g cross sections on the left, dotted lines refer to deviations on the right).

A detailed comparison of the major contributors to the differences can be carried out by collapsing the continuous-energy cross sections into the VITAMINJ 175-group structure. Relative deviations to Serpent results concerning ^{239}Pu and ^{241}Pu production and capture reactions are depicted in Figure 3 and Figure 4, respectively. It can be noted that significant differences appear in the unresolved resonance regions for both isotopes, being the URR boundaries marked. On the other hand, negligible differences appear outside this region in all cases. Specifically, KENO-VI is overestimating the production cross section in both cases while the capture is being underestimated. Then, the unresolved range treatment applied by each code leads to the large differences in the multiplication factor which has been previously observed.

In order to analyze the effect of the unresolved range treatment on the multiplication factor, calculations have been repeated by omitting the data embedded into the probability-tables (P-T) for this range. The results from these calculations are summarized in Table 2. Firstly, Serpent and MCNP-HZDR predicted identical results regarding the URR effect on the k_{inf} which is consistent since both cases are based in the same NJOY-processed library. Secondly, MCNP-CIEMAT shows a slightly larger URR effect compared to MCNP-HZDR that can be attributed to the processing of basic ENDF data. Furthermore, KENO significantly overestimates the URR effect with respect to Serpent and MCNP, i.e. 525 pcm in contrast to 50-100 pcm, which could be related to both the AMPX-formatted data processing and inherent Monte Carlo methods. In addition, all results are in a very good agreement when the P-T data are not considered which confirms that the URR treatment can explain the differences.
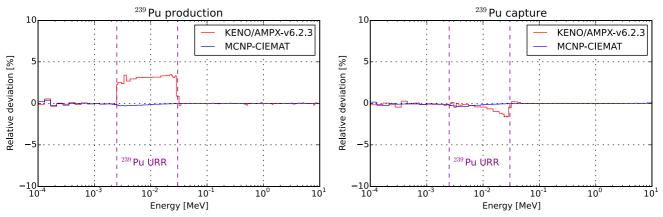

Figure 3: Relative deviations in ^{239}Pu production and capture microscopic cross section with respect to Serpent results collapsed into 175-groups.
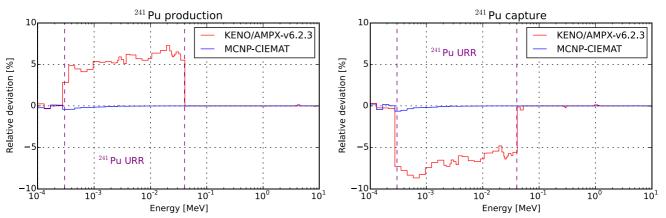

Figure 4: Relative deviations in ^{241}Pu production and capture microscopic cross section with respect to Serpent results collapsed into 175-groups.

Calculation	k_{inf} with P-T	k_{inf} without P-T	URR effect [pcm]	$\Delta\rho$ without P-T [pcm]
Serpent	1.31687(2)	1.31601(2)	50	reference
MCNP-HZDR	1.31685(5)	1.31599(5)	50	-1
MCNP-CIEMAT	1.31853(5)	1.31683(5)	98	47
KENO-VI	1.32607(2)	1.31689(3)	525	51

Table 2: Quantification of the unresolved resonance region effect on the multiplication factor predicted in each case and differences with respect to Serpent

For one-group cross sections, significant differences concerning the URR effect are obtained accordingly (see Figure 5). It can be seen that KENO-VI overestimates this effect compared to Serpent and MCNP for those isotope/reaction pairs which have been identified as the major contributors to the discrepancies.
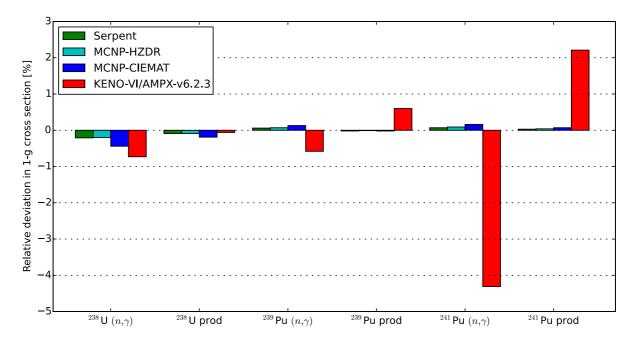

Figure 5: Effect of the unresolved resonance region on the one-group cross sections.

Updated ENDF/B-VII.1 library for KENO-VI SFR calculations

As detailed in the previous section, the application of the probability tables for the unresolved resonance region causes significant discrepancies between KENO-VI and Serpent and MCNP Monte Carlo codes. These differences are caused by differences in the generation of the applied nuclear data libraries. While Serpent and MCNP use data generated by NJOY, KENO-VI uses nuclear data processed by AMPX [15]. During the analysis of fast spectrum systems, it was discovered that the probability tables generated by AMPX included a normalization issue [16]. This issue has recently been fixed, and the next SCALE release (i.e. 6.3.0) will include nuclear data libraries that include corrected probability tables.

In addition to KENO-VI calculations using the released data library that include the normalization issue, KENO-VI calculation using a pre-release of the corrected ENDF/B-VII.1 data library was performed on the same simplified pin-cell benchmark.

Calculation	k_{inf} with P-T	k_{inf} without P-T	URR effect [pcm]	$\Delta\rho$ with P-T [pcm]	$\Delta\rho$ without P-T [pcm]
Serpent	1.31687(2)	1.31601(2)	50	reference	reference
MCNP-HZDR	1.31685(5)	1.31599(5)	50	-1	-1
MCNP-CIEMAT	1.31853(5)	1.31683(5)	98	96	47
KENO-VI/AMPX-6.2.3	1.32607(2)	1.31689(3)	525	527	51
KENO-VI/AMPX-6.3.0	1.31838(2)			87	

Table 3: Quantification of the unresolved resonance region effect on the multiplication factor predicted in each case and differences compared to Serpent.

Table 3 presents the results of the criticality calculations as well as the effect of the unresolved resonance range in all cases. Using the optimized SCALE library, k_{inf} shows a more reasonable agree-

ment compared to the other codes, decreasing the impact of the probability tables up to 87 pcm, which is slightly higher than Serpent but consistent with MCNP-CIEMAT. In all cases the reactivity differences are lower than 100 pcm, in contrast to the discrepancy of 527 pcm previously obtained.

Concerning the one-group collapsed cross sections, the optimized library shows a clear improvement with respect to the reference KENO-VI calculation. The cross sections related to the isotopes which were previously identified as major contributors to the differences show the following enhancements:

- ^{241}Pu one-group capture and production cross section differences compared to Serpent considerably decrease from 4.13% to 0.34% and from 2.37% to 0.19% respectively.

- The KENO-Serpent differences in ^{239}Pu one-group capture and production cross sections are reduced from 0.79% to 0.09% and from 0.51% to 0.12% respectively.

The improvement can be noticeably seen by collapsing the cross sections into the 175-group structure (see Figure 6 and Figure 7). As it can be seen, for production and capture cross sections of ^{239}Pu, differences with respect to Serpent are in a very good agreement with the MCNP-CIEMAT ones. In both cases, deviations are lower than 0.5% along the unresolved resonance range. On the other hand, also production and capture cross section of ^{241}Pu present an improvement although some noise profile remains. Nevertheless, those differences are lower than 1.7% along the range in contrast to the very close to 10% previously identified.
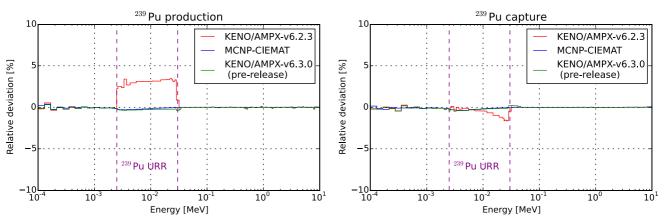

Figure 6: Relative deviations in ^{239}Pu production and capture microscopic cross section with respect to Serpent results collapsed into 175-groups.
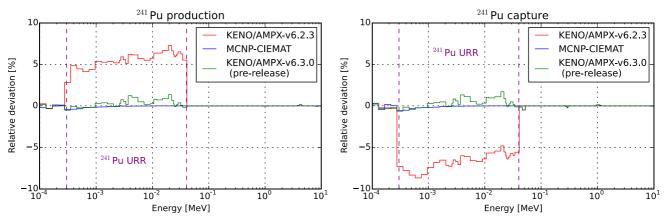

Figure 7: Relative deviations in ^{241}Pu production and capture microscopic cross section with respect to Serpent results collapsed into 175-groups.

In summary, the updated library significantly improves KENO-VI simulation for Sodium Fast Reactors solving the differences with respect to Serpent or MCNP previously observed.

Conclusions

A simplified pin-cell benchmark has been carried out in the frame of the ESFR-SMART project in order to provide insight into the discrepancies that KENO-VI exhibits when compared to other Monte Carlo codes for advanced fast reactor systems. Those deviations have appeared not only for Sodium Fast Reactors such as ASTRID, Superphénix or the optimized ESFR but also for the Lead-cooled Fast Reactors ALFRED and MYRRHA.

The three Monte Carlo codes, namely, KENO-VI, Serpent and MCNP were benchmarked in this work using the ENDF/B-VII.1 nuclear data library, AMPX-formatted for KENO-VI and NJOY processed for both Serpent and MCNP.

Criticality calculations have been performed, being the infinite multiplication factor predicted by KENO-VI around 500 pcm higher than the values predicted by Serpent and MCNP. Fission, production and capture cross sections for the main isotopes were collapsed into one-group in order to identify the major contributors to the discrepancies. Both ^{241}Pu and ^{239}Pu production and capture cross sections were identified as the most important contributors. By collapsing those cross sections into 175-group structure, it was concluded that differences are mainly due to the unresolved resonance region treatment. KENO-VI is considerably overestimating the effect of this region on the multiplication factor prediction with respect to both Serpent and MCNP. Calculations without the probability tables confirmed this statement.

The observed differences could be explained by a normalization issue in the generation of probability tables with AMPX for SCALE, which has recently been fixed. Significant enhancements regarding the effect of the unresolved range were observed when using a pre-release of the corrected ENDF/B-VII.1 library.

Regarding the results provided by Serpent and MCNP, a perfect agreement can be observed when using exactly the same processed library. Different options in the NJOY processing system to convert evaluated data into final application libraries lead to slight deviations.

This simplified benchmark exercise is therefore a good benchmark to check the impact of the URR in Monte Carlo simulations of fast reactors and to assess the adequacy of the processed continuous-energy libraries for best-estimate reactor calculations.

Acknowledgment

References

1) K. Mikityuk et al., "ESFR-SMART: new Horizon-2020 project on SFR Safety", In: Proceedings of Int. Conf. on Fast Reactors and Related Fuel Cycles: Next Generation Nuclear Systems for Sustainable Development, Yekaterinburg, Russia, June 26-29, 2017.

2) A. Ponomarev et al., "New Sodium Fast Reactor Neutronics Benchmark". In: Proceedings of the Int. Conf. on the Physics of Reactors (PHYSOR2018), Cancun, Mexico, April 22-26, 2018.

3) S. Bortot et al., "European benchmark on the ASTRID-like low-void-effect core characterization: neutronic parameters and safety coefficients". In: Proceedings of ICAPP2015, Nice, France, May 03-06, 2015.

4) P. Romojaro, "Sensitivity and uncertainty analysis of the ALFRED lead-cooled fast reactor using SCALE system", MSc Thesis, UPM, 2015.

5) CHANDA, 2013. EC Community Research and Development Information Service – CHANDA project (WWW Document), https://cordis.europa.eu/project/rcn/110083_en.html

6) P. Romojaro et al., "Nuclear data sensitivity and uncertainty analysis of effective neutron multiplication factor in various MYRRHA core configurations", *Annals of Nuclear Energy*, **101**, 330-338, 2017.

7) L. B. Levitt, "The Probability Table Method for Treating Unresolved Neutron Resonances in Monte Carlo Calculation", *Nuclear Science and Engineering*, **49**, 450-457 (1972).

8) R. D. Mosteller and R. C. Little, "Impact of MCNP Unresolved Resonance Probability-Table Treatment on Uranium and Plutonium Benchmarks". In: Proceedings of the ICNC99, Versailles, France, September 20-24, 1999.

9) B.T. Rearden et al., "Monte Carlo capabilities of the SCALE code system", *Annals of Nuclear Energy*, **82**, 130-

141, 2015.

10) B.T. Rearden and M. A. Jesse, "SCALE Code System (Version 6.2)". ORNL/TM-2005/39, Version 6.2, Oak Ridge National Laboratory, 2016.

11) M. B. Chadwick et al., "ENDF/B-VII.1 Nuclear Data for Science and Technology: Cross Sections, Covariances, Fission Product Yields and Decay Data", *Nuclear Data Sheets*, **112**, 2887-2996, 2011.

12) D. B. Pelowitz et al., "MCNP6 TM USER'S MANUAL Code Version 6.1.1beta". Los Alamos National Laboratory, Report LA-CP-14-00745, 2014.

13) D. W. Muir et al., "The NJOY Nuclear Data Processing System, Version 2016". Los Alamos National Laboratory, Report LA-UR-17-20093, 2016.

14) J. Leppänen et al., "The Serpent Monte Carlo code: Status, development and applications in 2013". *Annals of Nuclear Energy*, **82**, 142-150, 2013.

15) D. Wiarda et al., "AMPX-6: A Modular Code System for Processing ENDF/B". Oak Ridge National Laboratory, Oak Ridge, TN. Available from Radiation Safety Information Computational Center as CCC-834, 2016.

16) K. S. Kim et al., "The AMPX/SCALE Multigroup Cross Section Processing for Fast Reactor Analysis". In: Proceedings of PHYSOR2018, Cancun, Mexico, April 22-26, 2018.